# Reactions of self-healing agents and the chemical binding of aggressive ions in sea water Thermodynamics and kinetics

Wu, Xintong; Huang, Haoliang; Liu, Hao; Hu, Jie; Wei, Jiangxiong; Jiang, Zhengwu; Ye, Guang; Yu, Qijun; Lothenbach, Barbara

**DOI**
10.1016/j.cemconres.2021.106450

**Publication date**
2021

**Document Version**
Accepted author manuscript

**Published in**
Cement and Concrete Research

**Citation (APA)**
Wu, X., Huang, H., Liu, H., Hu, J., Wei, J., Jiang, Z., Ye, G., Yu, Q., & Lothenbach, B. (2021). Reactions of self-healing agents and the chemical binding of aggressive ions in sea water: Thermodynamics and kinetics. *Cement and Concrete Research*, *145*, 1-13. Article 106450. https://doi.org/10.1016/j.cemconres.2021.106450

# REACTIONS OF SELF-HEALING AGENTS AND THE CHEMICAL BINDING OF AGGRESSIVE IONS IN SEA WATER: THERMODYNAMICS AND KINETICS

Xintong WU (1), Haoliang HUANG (1), (2)*, Hao LIU (1), Jie HU (1), (2), Jiangxiong WEI (1), (2), Zhengwu Jiang (3), Guang YE (4), Qijun YU (1), (2), Barbara Lothenbach (5)

(1) School of Materials Science and Engineering, South China University of Technology, Guangzhou, China

(2) Guangdong Low Carbon Technologies Engineering Centre for Building Materials, Guangzhou, China

(3) School of Materials Science and Engineering, Tongji University, Shanghai, China

(4) Microlab, Faculty of Civil Engineering and Geoscience, Delft University of Technology, Delft, The Netherlands.

(5) EMPA, Laboratory for Concrete and Construction Chemistry, 8600, Dübendorf, Switzerland

**Abstract:** New self-healing agents that can chemically bind seawater ions invading cracked cementitious materials were proposed. The potential of self-healing and binding of seawater ions were investigated by thermodynamic modeling. It was found that CaO-$NaAlO_2$ and CaO-metakaolin agents can have $Cl^-$, $SO_4^{2-}$ and $Mg^{2+}$ chemically bound by reacting with sea water to form Friedel's salt, Kuzel's salt, ettringite and hydrotalcite. The removal of $Cl^-$ from seawater firstly increased and then decreased with the increase of Ca/Al molar ratio in both agents, while the

removal of $Mg^{2+}$ and $SO_4^{2-}$ were hardly influenced and approximated 100%. Because $NaAlO_2$ dissolves and releases $Al(OH)_4^-$ rapidly, precipitates binding $Cl^-$, $SO_4^{2-}$ and $Mg^{2+}$ were formed fast. In comparison, the reaction of metakaolin binding aggressive ions occurred after 3 days. Because of the faster reaction and the capacity to make $[Cl^-]/[OH^-]$ lower in the solution, $CaO\text{-}NaAlO_2$ would be more efficient for self-healing and mitigating reinforcement corrossion than CaO-metakaolin.

**Keywords: self-healing, thermodynamic modeling, ion binding, marine environment, cementitious materials**

## 1. INTRODUCTION

The occurrences of cracks usually take place in reinforced concrete elements. In the concrete structures in marine environments, such cracks can become pathways for ingress of different ions, such as $Cl^-$, $SO_4^{2-}$ and $Mg^{2+}$, causing deterioration of the concrete structures. Actually, concrete is able to heal cracks autogenously to some extent. A potential solution to improve the durability of reinforced concrete in marine environments is to support the self-healing of cracks by using chemical agents.

Self-healing of cracks in cementitious material has attracted significant attention in recent years [1-5]. It was found that environmental factors, in particular the ions from the environment, significantly affected the self-healing process and efficiency [1]. It was reported that autogenous self-healing of cracks in a marine environment is promoted by $Mg^{2+}$ in the sea water [6, 7]. Compared to autogenous self-healing in fresh water, autogenous self-healing in sea water can enhance the closure ratio of a surface crack with an initial width of 400 μm by 37% for a healing period of 7 days [7]. However, it must be emphasized that there are multiple aggressive ions in the marine environments, such as $Cl^-$, $SO_4^{2-}$ and $Mg^{2+}$. While these ions might contribute to the self-healing they can also decrease the durability of reinforced concrete as they lead to weakening of the concrete cover and corrosion of steel bars [8-10]. It is conceivable that once cracks appear, the aggressive ions can invade faster through these cracks. Therefore, an ideal self-healing agent to improve the durability performance of cracked reinforced concrete in a marine environment should not only

promote the self-healing of cracks (to prevent the further ingress of aggressive ions), but also be able to "capture" these aggressive ions that have already invaded the cracks.

In the presence of $Ca^{2+}$ and $Al(OH)_4^-$, $Cl^-$, $SO_4^{2-}$ and $Mg^{2+}$ are known to precipitate as Friedel's salt ($3CaO \cdot Al_2O_3 \cdot CaCl_2 \cdot 10H_2O$), ettringite ($3CaO \cdot Al_2O_3 \cdot 3CaSO_4 \cdot 32H_2O$) and hydrotalcite ($4MgO \cdot Al_2O_3 \cdot 10H_2O$) [11-13], which means that $Cl^-$, $SO_4^{2-}$ and $Mg^{2+}$ in the crack can be chemically bound. Simultaneously, the crack can be filled by such precipitates. It is well known that calcium is one of the main elements in Portland cement-based materials. According to a previous study [14], unhydrated cement and portlandite with a relatively high solubility results in the diffusion of $Ca^{2+}$ ions into the crack. In addition, $Al(OH)_4^-$ ions can be supplied by Al-rich materials, such as slag and metakaolin, which can be added directly by blending or after encapsulation. Thus in a next step the binding efficiency of $Cl^-$, $SO_4^{2-}$ and $Mg^{2+}$, and the volume of precipitates formed in sea water need to be investigated as a function of the moles of $Ca^{2+}$ and $Al(OH)_4^-$ ions, and their molar ratio.

In this study, the appropriate moles of $Ca^{2+}$ and $Al(OH)_4^-$ ions, as well as their molar ratio, were determined by thermodynamic modeling for the self-healing of cracks and the chemical binding of $Cl^-$, $SO_4^{2-}$ and $Mg^{2+}$ ions from sea water. The volume of relevant precipitates and the corresponding binding efficiency of the aggressive ions in sea water as a function of the masses and ratio of $Ca^{2+}$ and $Al(OH)_4^-$ ions were predicted. Moreover, in order to evaluate the thermodynamic modeling results and obtain further information on the kinetics of the binding reactions, $CaO\text{-}NaAlO_2$ and CaO-metakaolin, the agents that provide $Ca^{2+}$ and $Al(OH)_4^-$ were reacted with simulated sea water. The mineralogy of the reaction products was determined by means of X-ray diffraction (XRD). The relative content of Cl, S and Mg chemically bound in the reaction products were quantified by X-ray fluorescence analysis (XRF). The change in concentrations of $Mg^{2+}$, $SO_4^{2-}$, and $Cl^-$ in simulated sea water as a function of reaction time was monitored by means of Ion Chromatography (IC) and Inductively Coupled Plasma (ICP). Based on these results,

appropriate self-healing agents can be developed and used to manufacture artificial aggregates [15] or encapsulated in polymeric capsules [16, 17] and added into concrete deliberately.

## 2. MATERIALS AND METHODS

### 2.1 Thermodynamic modeling

Thermodynamic modeling was performed with the software GEMS 3.5, in which Gibbs energy minimization was adopted to calculate the mass and volume of equilibrium phase assemblages and the equilibrium ion concentrations from the total bulk elemental composition. The CEMDATA18 database [18] for cementitious materials was used. The related chemical reactions and the corresponding equilibrium constants $K_{so}$ are listed in Table 1.

The modeling simulated the reactions taking place after the self-healing agents were mixed with 100 mL seawater. The ratio between the mass of self-healing agent and the mass of seawater ranged from 0.02 to 0.3. Total moles of ions released from self-healing agents can be calculated according to the chemical compositions of the self-healing agents. Total moles of ions in seawater can be determined according to the ion concentrations of seawater given in Section 2.2. These ion compositions should be input into GEMS 3.5 as initial conditions. Moreover, in the simulation the temperature, at which the reactions of self-healing agents in seawater take place, was assumed to be 25℃.

### 2.2 Experiments for studying the reactions between the self-healing agents and simulated sea water

2.2.1 Materials and sample preparation

In order to evaluate the thermodynamic modeling results and obtain further information on the kinetics of the reactions, the self-healing agents were directly mixed with simulated sea water for reactions. Two types of self-healing agent, i.e. CaO-$NaAlO_2$ and CaO-metakaolin, were prepared from CaO, $NaAlO_2$ and metakaolin.

The purity of these chemical agents was higher than 99.7%. By changing the mass percentages of CaO in the self-healing agent mixtures, the Ca/Al molar ratios can be modified. According to the thermodynamic results in Section 3.1, the Ca/Al in the self-healing agents used for experimental studies was set to be 3 and 5.

By following the literature [7], sea water was prepared by using the chemical agents listed in Table 2. The purity of all these chemical agents was higher than 99.7%. The concentration of the main ions in simulated sea water is presented in Table 2.

The ratio between the mass of self-healing agents to the mass of simulated sea water was set to be 0.2. After the agents were mixed with simulated sea water for 1 minute, the mixtures in containers were sealed with plastic sheet with very small holes so that water evaporation was hindered but the air still accessed. The mixtures were cured in a room with a temperature of 20±1℃. At 0.5, 1, 3, 7, 14 and 28 days, the mixtures were centrifuged to separate the solid phase from the solution, respectively. After that, the solid phases were washed 3 times with ethanol and dried at 40℃ in an oven until the weight was constant. Finally, the dried solid phases were grounded with agate mortar and pestle set to pass 200-mesh sieve.

2.2.2 Characterization of the reaction products of the self-healing agents

In order to determine the crystalline phases in the reaction products, X-ray Diffraction (XRD) analysis was performed on a X'Pert PRO X-ray diffractometer by using Cu Kα as a radiation source. The samples were measured between 5°2θ and 90°2θ with a step size of 0.033°2θ. The contents of each crystalline phases in reaction products of self-healing agents reacted with seawater for 28 days were quantified based on Rietveld method. In order to guarantee the accuracy of the quantification, the analysis was not accomplished until a sig parameter was between 1-2 and, simultaneously, the $R_w$ parameter was less than 15.

For self-healing agent CaO-matakaolin XRD can hardly provide information for gel reaction products, i.e. C-S-H. Therefore, reaction products of CaO-matakaolin, which was mixed and reacted with seawater for 28 days, were characterized by means of EDS. Before

testing, powders of reaction products were impregnated with epoxy. After the epoxy was hardened, the samples were sequently ground with sandpapers P320, P500, P1200 and P4000. To analyze the chemical elements of the reaction products, random points on the surfaces of the reaction products were tested by EDS. For the analysis, a beam with accelerating voltage of 20 kV was used and the magnification was 400X and 500X.

X-ray Fluorescence (XRF) analysis on the reaction products were carried out using Axios Pw 4400, PaNalytical B.V, with Rh as radiation source and an accuracy of 0.05%. According to XRF results, the binding efficiency (BE) of ions by the self-healing agents can be determined with Equation 1.

$$BE = \frac{m(Cl,S,Mg)}{m(CaO+SiO_2+Al_2O_3)} \times 100\% \quad (1)$$

where $m$ refers to the mass percentage of compositions determined by XRF.

The volume increase of the healing agents facilitates the self-healing of cracks. Thus, the volume of solid phases as a function of reaction time was measured with pycnometer to evaluate the potential healing capacity of the self-healing agents and compared with the thermodynamic modeling results.

2.2.3 Evaluation on the removal of aggressive ions from simulated sea water by the self-healing agents

The concentrations of sulfate and chloride in the solution obtained after the mixing of self-healing agents with the simulated sea water were measured by using ion chromatography (IC). For the measurements, 1mM $NaHCO_3$ solution at a flow rate of 1mL/min was used as eluent. The volume of the sample injection loop was 1mL. In addition, the concentrations of magnesium in the solutions at different reaction time were measured by inductively coupled plasma optical emission spectrometry (ICP-OES). Based on the concentrations at different reaction times, the removal efficiency of the self-healing agents was determined as follows:

$$IR = \frac{C_i - C_t}{C_i} \times 100\% \quad (2)$$

where $C_i$ is the initial concentration in simulated sea water and $C_t$ is the concentration in the solution after a reaction period of t.

## 3. RESULTS AND DISCUSSION

### 3.1 Thermodynamic modelling results on the reactions between self-healing agents and sea water

#### 3.1.1 Phase assemblages of the self-healing agents mixed with sea water

For the $CaO\text{-}NaAlO_2$ agent, Friedel's salt, ettringite, hydrotalcite and portlandite are the main precipitates formed at low dosages of self-healing agent as shown in Fig. 1. Ettringite is only present if the ratio between the mass of $CaO\text{-}NaAlO_2$ agent and the mass of sea water is less than 0.1 at molar Ca/Al =3 and 0.14 at molar Ca/Al =5. If the ratio between the mass of $CaO\text{-}NaAlO_2$ agent and the mass of sea water increases, the volume of precipitates also increases and the mineralogy changes. Ettringite disappears and the volume fraction of Friedel's salt decreases, while Kuzel's salt forms. Moreover, for the $CaO\text{-}NaAlO_2$ agent with Ca/Al of 3, $C_3AH_6$ is formed when the ratio between the mass of $CaO\text{-}NaAlO_2$ agent and the mass of sea water is larger than 0.18 at molar Ca/Al=3 and larger than 0.26 at Ca/Al of 5. The percentage of portlandite in the mixture of sea water and $CaO\text{-}NaAlO_2$ agent with Ca/Al of 5 is larger than that with Ca/Al of 3, due to the higher availability of CaO at Ca/Al of 5.

For the mixture of CaO-metakaolin agent and sea water, in addition to Friedel's salt and ettringite, C-S-H and straetlingite ($CaAl_2Si_2O_8$) are expected to be formed. It is worth noting that at Ca/Al molar ratio of 3 (see Fig. 2 (a)) portlandite is absent, while at Ca/Al molar ratio of 5 (see Fig. 2 (b)) portlandite is expected, as in the presence of metakaolin C-S-H and strätlingite can bind additional calcium.

Fig. 1 Phase assemblages in the mixture of $CaO\text{-}NaAlO_2$ and 100 ml sea water based on thermodynamic modeling: (a) with Ca/Al molar ratio of 3; (b) with Ca/Al molar ratio of 5

Fig. 2 Phase assemblages in the mixture of CaO-metakaolin and 100 ml sea water based on thermodynamic modeling: (a) with Ca/Al molar ratio of 3; (b) with Ca/Al molar ratio of 5

As discussed above, the Ca/Al in the ion-binding agent, related to the mass percentage of CaO in the agent, has a significant effect on the mineralogy of the phase assemblages, and thus a significant effect on the binding of sulfate, chloride and magnesium present in sea water. Thus, the effect of changing Ca/Al on the phase assemblages was investigated. Fig. 3 and 4 show that the mineral composition of the reaction products changes with Ca/Al molar ratio in the self-healing agents. In general, an increase of Ca/Al provides more CaO and less $Al_2O_3$. Therefore, the volume percentage of phases containing Al decreases and the volume of portlandite increases with the increase of Ca/Al. By comparing Fig. 4 with Fig. 3, it can be seen that at a higher ratio, i.e. 0.3, between the mass of self-healing agents and the mass of sea water, the total volume of reaction products is significantly larger than the volume at 0.2.

Fig. 3 Phase assemblages in the mixture of 100 ml sea water and 20 g self-healing agents with various Ca/Al based on thermodynamic modeling: (a) CaO-$NaAlO_2$; (b) CaO-metakaolin. Fs: Friedel's salt

Fig. 4 Phase assemblages in the mixture of 100 ml sea water and 30 g self-healing agents with various Ca/Al based on thermodynamic modeling: (a) CaO-$NaAlO_2$; (b) CaO-metakaolin. Fs: Friedel's salt; Ks: Kuzel's salt

### 3.1.2 Removal efficiency of chloride, sulphate and magnesium from solution.

As discussed above, thanks to the formation of Friedel’s salt, ettringite and hydrotalcite after the self-healing agents react with sea water, chloride, sulphate and magnesium in the sea water can be chemically bound. From this point of view, they are removed from the solution.

As shown in Fig. 5 (a), in general, the removal efficiency of chloride from sea water increases linearly with the increase of the amount of self-healing agents. Only for the CaO-$NaAlO_2$ agent with Ca/Al of 3, the removal efficiency of chloride reaches a maximum of 80% when the ratio between the mass of agent and the mass of sea water is 0.2. Moreover, the slope of the lines for Ca/Al of 3 is larger than that of 5, indicating a higher chloride uptake at Ca/Al of 3 than at 5.

Fig. 5 (b) and (c) show that nearly 100% of sulphate and magnesium can be removed even at a low ratio between the mass of self-healing agent and the mass of sea water, indicating a higher binding efficiency of sulfate and magnesium than of chloride. A "valley" is observed in the removal efficiency curves of $SO_4^{2-}$ in the four series of self-healing agent (see Fig. 5 (b)) corresponding to the transition of ettringite to the Kuzel's salt shown in Fig. 1 and 2, which demonstrates that from a thermodynamic point of view ettringite binds sulfate stronger than Kuzel's salt.

Fig. 5 Removal efficiency of ions as a function of ratio between the mass of agent to the mass of sea water based on thermodynamic modeling: (a) $Cl^-$; (b) $SO_4^{2-}$; (c) $Mg^{2+}$ in sea water. C/A means Ca/Al molar ratio.

Fig. 6 plots the removal efficiency of chloride, sulfate and magnesium in sea water as a function of Ca/Al molar ratio of the self-healing agent. It can be seen that the chloride removal increases to a maximum when the Ca/Al molar ratio of self-healing agents ranges from 3 to 5, while decreases when the Ca/Al increases further (see Fig. 6 (a)). In case the ratio between the mass of self-healing agent and the mass of sea water equals to 0.2 or 0.3, the maximum chloride removal efficiency is less than 90% for both self-healing agents. In contrast, as shown in Fig. 6 (b), the removal efficiency of sulfate is very high for both agents, near 100% for the CaO-metakaolin and slightly lower for CaO-$NaAlO_2$ when the Ca/Al ratio is higher than 3. It is interesting to note that for CaO-$NaAlO_2$ agent this sulfate removal efficiency becomes much lower when the Ca/Al is smaller than 2, which is important information for designing the self-healing agent. Fig. 6 (c) shows that the removal efficiency for magnesium is not

254 influenced by Ca/Al and approximates 100%.

255 It must be mentioned that in the modeling regarding the agents with metakaolin,
256 the physical binding of chloride by C-S-H was not considered. To target at an
257 optimization on the self-healing agent that can bind these ions as stably as possible,
258 only chemical binding was taken into account in the thermodynamic modeling.

259

260 Fig. 6 Removal efficiency of chloride, sulfate and magnesium in sea water as a
261 function of Ca/Al in self-healing agents based on thermodynamic modeling: (a) $Cl^-$; (b)
262 $SO_4^{2-}$; (c) $Mg^{2+}$. SH/SW refers to the ratio between the mass of self-healing agent and
263 the mass of sea water.

### 3.1.3 The pH in the sea water mixed with the self-healing agents

Fig. 7 shows the calculated pH values in the sea water mixed with different amount of self-healing agents based on thermodynamic modeling. The pH value increases with the amount of self-healing agents and is generally higher for the CaO-$NaAlO_2$ than for CaO-metakaolin agent.

Fig.7 pH value as a function of the ratio between the mass of agent to the mass of sea water based on thermodynamic modeling. C/A means Ca/Al molar ratio.

The pH value plotted as a function of Ca/Al for the CaO-$NaAlO_2$ agent decreases from 14 to 13.5 with an increase of Ca/Al from 1 to 10 (see Fig. 8). With an increase of Ca/Al, less $Na^+$ is provided to the system by the self-healing agent, resulting in a decrease of pH value. For the sea water mixed with CaO-metakaolin agent, the pH is lower than that with CaO-$NaAlO_2$ agent and increases strongly when Ca/Al increases from 1 to 3, and remains higher than 12.5 at Ca/Al > 3. The solid phase assemblages shown in Fig. 3 (b) and 4 (b) indicate the absence of portlandite in the mixture of CaO-metakaolin agent at Ca/Al < 3 and sea water. Moreover, strätlingite and Ca/Si C-S-H are able to bind some alkali ions, also leading to an lower pH value for Ca/Al ranging from 1 to 3.

Fig. 8 pH value in sea water mixed with self-healing agent with various Ca/Al based on thermodynamic modeling. SH/SW refers to the ratio between the mass of self-healing agent and the mass of sea water.

The pH value, together with the chloride concentration, has a significant influence on corrosion of reinforced concrete. In a non-damaged concrete, steel reinforcements remain passive due to high alkalinity of pore solution (pH＞13) [20]. In cracked concrete, the easy ingress of $Cl^-$ can cause depassivation of reinforcement even at a high pH in pore solution. Therefore, a critical corrosion ratio between the

concentration of $Cl^-$ and the concentration of $OH^-$ ($[Cl^-]/[OH^-]$) in pore solution is often used to evaluate the corrosion initiation of reinforcement, which is influenced by $Cl^-$ concentration and pH. Higher concentrations of chlorides and sulphates relative to the hydroxyl concentration can increase the corrosion rate of carbon steel [21]. Selected thresholds for corrosion initiation are $[Cl^-]/[OH^-] > 0.6$ and $[SO_4^{2-}]/[OH^-] > 1.5$ [22, 23] and shown in Fig. 9. It can be seen that the ratio between the mass of self-healing agent and the mass of sea water, as well as the Ca/Al molar ratio in the agent, have significant influence on the $[Cl^-]/[OH^-]$ value (see Fig. 9 (a)). For $CaO\text{-}NaAlO_2$ agent, mixed with sea water at a mass ratio of 0.2, the $[Cl^-]/[OH^-]$ value is lower than 0.6 when Ca/Al molar ratio is between 1 and 5. When the $CaO\text{-}NaAlO_2$ agent mixed with sea water at a mass ratio of 0.3, the Ca/Al molar ratio in the agent that leads to a $[Cl^-]/[OH^-]$ value lower than 0.6 ranges from 1 to 9. For CaO-metakaolin agent mixed with sea water at a mass ratio of 0.3, when the Ca/Al molar ratio is between 3 and 6, the $[Cl^-]/[OH^-]$ value is also lower than 0.6. However, when the CaO-metakaolin agent mixed with sea water at a mass ratio of 0.2, the $[Cl^-]/[OH^-]$ value is hardly lower than 0.6 no matter what the Ca/Al molar ratio is. In term of $[SO_4^{2-}]/[OH^-]$, both agents with Ca/Al molar ratio larger than 1 can lead to a value of $[SO_4^{2-}]/[OH^-]$ lower than 1.5 (see Fig. 9 (b)).

Note that the use of such threshold values is a simplification as the corrosion rate and extent is influenced by many factors. Based on those ratios as an indicator for the corrosion risk of steel bars, a higher pH value and chloride/sulfate removal efficiency can decrease the rebar corrosion risk. Therefore, according to the thermodynamic results, the self-healing agents should not only remove the chloride and sulfate from the crack solution, but also increase the pH, so as to have potential to protect rebar from corrosion induced by the chloride and sulfate from sea water.

Fig. 9 Ratios between concentration of $Cl^-$ or $SO_4^{2-}$ and the concentration of $OH^-$: (a) $Cl^-/OH^-$, (b) $SO_4^{2-}/OH^-$. SH/SW refers to the ratio between the mass of self-healing agent and the mass of sea water.

### 3.2 Experimental results on kinetics of the reactions between self-healing agents and simulated sea water

#### 3.2.1 Mineralogy of the reaction products based on XRD results

Fig. 10 shows the XRD patterns of the solid phases obtained after reactions of the self-healing agents with simulated sea water for different periods. After the reaction of CaO-$NaAlO_2$ agent with sea water, the solid phases mainly contained Friedel's salt, $SO_4$-$CO_3$-AFm, hydrotalcite and portlandite (see Fig. 10 (a) (b)). It can be seen that $C_3AH_6$ occured at 12 hours of the reaction between CaO-$NaAlO_2$ agent and sea water. However, it disappeared thereafter and the mineral composition in the solid phases did not change with reaction times anymore, indicating that self-healing agent can completely react with sea water before 1 day. By comparing Fig. 10 (a) with (b), it is found that change of Ca/Al in CaO-$NaAlO_2$ agent had no influence on the mineral composition of the reaction products.

Also, for the CaO-metakaolin agent with Ca/Al of 5 reacting with sea water, the mineral compositions of solid phases changed with reaction times. As shown in Fig. 10 (c), diffraction peaks of Friedel's salt and hydrotalcite were not obvious at 1 day, while those of portlandite were distinct. As the reactions proceeded, the diffraction peaks of Friedel's salt and hydrotalcite became more distinct. This is related to the relatively slow reaction between metakaolin and the $Ca(OH)_2$ in the system.

Table 3 lists the contents of the crystalline phases in reaction products of self-healing agents reacted with seawater for 28 days. It was found that for CaO/$NaAlO_2$ agent, the total content of AFm phases decreased as the Ca/Al increased from 3 to 5, while the content of $Ca(OH)_2$ by about 75%. For CaO/metakaolin agent, AFm phases accounts for about 50% of the reaction products. It should be mentioned that the high content of $CaCO_3$ in the reaction products of CaO/metakaolin agent was due to the carbonation of $Ca(OH)_2$ during the sample preparation.

The detection of Friedel's salt and hydrotalcite by XRD was consistent with the thermodynamic results shown in section 3.1. However, the simulated Kuzel's salt was not detected. Moreover, according to the experimental results $SO_4^{2-}$ was not bound in Kuzel's salt, but in $SO_4$-$CO_3$ AFm ($Ca_4Al_2O_6$ $(CO)_{0.67}$ $(SO_3)_{0.33}\cdot 11H_2O$, see Fig. 10),

which was not predicted by thermodynamic modeling. Calcite was also detected in the late stage of reactions. It must be mentioned that the modeling was based on thermodynamic theory. Mineralogy of reaction products were calculated based on the chemical species from complete dissolutions of self-healing agents and related thermodynamic equilibria. However, kinetics of the reactions between self-healing agents and seawater was ignored. In particular, dissolution rate of each mineral in the self-healing agents is different, which can lead to a different mineralogy of reaction products from the thermodynamic modeling results. However, thermodynamic modeling can still provide useful information for the design of such new self-healing agents.

Fig. 10 XRD patterns of solid phases obtained after the reaction of the self-healing agent with sea water: (a) CaO-$NaAlO_2$ agent with Ca/Al of 3; (b) CaO-$NaAlO_2$ agent with Ca/Al of 5; (c) CaO-metakaolin agent with Ca/Al of 5. For reactions, the ratio between the mass of self-healing agent and the mass of sea water was 0.2.

Fig. 11 shows point analysis results of the samples obtained by plotting atomic ratio of Si/Ca against Al/Ca. Tie lines were drawn from the cloud of C-S-H points and different phases of known theoretical compositions. The points near the tie lines correspond to a binary mixture of C-S-H and phase along the line [24]. Therefore, it can be deduced that in addition to AFt and AFm, C-S-H appears in the reaction products of CaO-matakaolin.

Fig. 11 EDS point analysis of reaction products of CaO-metakaolin reacted with seawater for 28 days. For the reaction, the ratio between the mass of self-healing agent and the mass of sea water was 0.2.

### 3.2.2 Ion removal based on solution concentrations

The concentrations of sulfate and chloride in the solution obtained after the mixing of self-healing agents with the simulated sea water were adopted to calculate the ion removal efficiency according to Equation 2. Fig. 12(a) shows that the removal

efficiency of chloride from sea water by the CaO-$NaAlO_2$ agent reached 45% for a reaction period of 0.5 day. After that, the removal efficiency fluctuated around this value. In comparison, the removal efficiency of chloride ion by the CaO-metakaolin agent with Ca/Al of 5 increased gradually and reached the maximum value, i.e. 50%, at 14 days, which was due to the slower metakaolin reaction. As shown in Fig. 12(a), the experimentally determined removal efficiencies were lower than the thermodynamic modeling results by 5% to 10%. Nevertheless, these differences still show a satisfactory agreement.

Fig. 12(b) shows that the removal efficiency of sulfate by the CaO-metakaolin agent with Ca/Al of 5 can reach 100% at a reaction time of 3 days, which is consistent with the modeling results. In contrast, the experimentally observed sulfate removal efficiency of the CaO-$NaAlO_2$ agent with Ca/Al of 3 and 5 only reached 60% at 0.5 day and longer. This is clearly lower than the modeling result. This could be related to a suppression of sulfate uptake by Kuzel's salt and $SO_4$-AFm at very high pH values up to 14, which is not sufficiently accounted for in the available thermodynamic models developed based on the data measured under a pH of 11 to 12.5 [25]. In fact, for the metakaolin sample with a lower pH value, i.e. about 13 (see Fig. 7), the prediction and measurements agree well.

In addition, as shown in Fig. 12(c), the removal efficiency of magnesium by self-healing agents reached 100% rapidly at the reaction time of 0.5 day, which compares well with the modeling result.

Fig. 12 Removal efficiency of aggressive ions in sea water after reaction with self-healing agents for different periods: (a) $Cl^-$; (b) $SO_4^{2-}$; (c) $Mg^{2+}$. C/A means Ca/Al molar ratio.

### 3.2.3 Ion binding observed by XRF analysis

By means of XRF, the mass ratio of chloride, sulfate and magnesium bound in the self-healing agents were determined and plotted in Fig. 13, compared with the results of thermodynamic modelling. It can be seen that although there is some difference

between the modeling results and the experimental results, the modeling can still provide information on the difference of ion binding abilities between the various self-healing agents. It should be mentioned that the relative mass percentages of ions bound in the solid phases were very low, only 6% to 9% for chloride and less than 2% for sulfate and magnesium. It is possible that the difference between the modeling results and the experimental results are partially caused by experimental errors as the relative mass percentages of ions in the solid phases are relatively low.

For the CaO-$NaAlO_2$ agent, the binding of aggressive ions reached the maximum value at a reaction time of 12 hours as $NaAlO_2$ dissolved rapidly in water and released $Al(OH)_4^-$ to make precipitates, i.e. Friedel's salt, AFm and hydrotalcite, formed immediately. Therefore, chloride, sulfate and magnesium were bound within a short period after the mixing of sea water with CaO-$NaAlO_2$ agent. In comparison, because of the slower reactions of CaO-metakaolin, the binding of these aggressive ions increased gradually until a reaction time of 14 days, which is consistent with the results on ion removal efficiency in Section 3.2.2.

It is interesting to notice that the binding of aggressive ions by CaO-$NaAlO_2$ agent decreased slightly after 3 days, and then remained at the similar level. This phenomenon was more obvious for the Ca/Al molar ratio of 3. This may be caused by the fast precipitation in these systems, which can lead to a strong co-precipitation of different ions, while a ripening of the solids with time can result in a partial release of such co-precipitated ions [26, 27]. No such phenomenon was observed for the slower reacting CaO-metakaolin agent.

Fig. 13 Aggressive ions binding efficiency in reaction products: (a) $Cl^-$; (b) $SO_4^{2-}$; (c) $Mg^{2+}$. C/A means Ca/Al molar ratio.

### 3.2.4 Volume increase of solid phases after reactions of self-healing agents with simulated sea water

The volume of the solid phase at different reaction periods was measured by a pycnometer. For the CaO-$NaAlO_2$ agent mixed with sea water, the volume of the solid

phase increased dramatically within the first 12 hours and remained stable thereafter. As mentioned above, $NaAlO_2$ dissolved rapidly in water and released $Al(OH)_4^-$. Thus precipitates binding aggressive ions in synthetic water were formed very fast. Therefore, the volume of the solid phase increased within the first 12 hours after CaO-$NaAlO_2$ agent was mixed with sea water, while little change occurred afterwards. The final increase ratio of CaO-$NaAlO_2$ agent with Ca/Al of 5 was smaller than that of the agent with Ca/Al of 3, which agrees with the sequence predicted by thermodynamic modelling.

As shown in Fig. 14, there were two stages for the volume increase of CaO-metakaolin agent with Ca/Al of 5 after mixed with sea water. The solid phase volume increased significantly within the first 12 hours after the CaO-metakaolin agent was mixed with sea water. After that, the increase slowed down up to 3 days but occured again between 3 and 7 days. After a reaction time of 7 days, the volume increase ratio reached 2.2 and remained stable. According to the XRD results in Fig. 9, portlandite was the main reaction product of the CaO-metakaolin agent mixed with sea water after 1 day, which seems to cause the first volume increase, as the hydration of lime into $Ca(OH)_2$ resulted in a significant volume increase [28]. After longer reaction times (> 3 days), metakaolin reacted significantly and Friedel's salt, Kuzel's salt, hydrotalcite and C-S-H were formed (see Fig. 10). The formation of these mineral which contain significant amounts of water in their structure was accompanied by volume increase [29]. Thus, the slow reaction of metakaolin and formation of Friedel's salt, Kuzel's salt, hydrotalcite and C-S-H contributed to the later volume increase up to 7 days. The final volume increase ratio of CaO-metakaolin agent in sea water determined experimentally compared reasonably well with the thermodynamic modeling result. Moreover, the experimental finding that both CaO-$NaAlO_2$ agents had smaller volume increases than CaO-metakaolin agent is consistent with the thermodynamic modelling.

Fig. 14 Volume increase ratio of self-healing agents mixed with simulated sea water. C/A means Ca/Al molar ratio.

### 3.2.5 Discussion on the self-healing efficiency: crack closure and binding of aggressive ions

As demonstrated above, the volume increase ratio of CaO-$NaAlO_2$ is lower than that of CaO-metakaolin self-healing agent (see Fig. 14). However, for hindering the ingress of aggressive ions into the crack, not only the crack filling, but also the distribution of precipitates in the crack space is important. As addressed in a previous study [7], where encapsulated CaO-metakaolin agent with Ca/Al of 3 was used as self-healing agent, brucite was the main mineral formed at the crack surfaces, while Friedel's salt and hydrotalcite were mainly formed inside the capsule, as the mobility of $Al(OH)_4^-$ (and $H_2SiO_4^{2-}$) is much lower than that of other ions in the system. Moreover, the solubility of Friedel's salt and hydrotalcite is much lower than that of portlandite or brucite. Therefore, Friedel's salt and hydrotalcite were formed locally inside the broken capsule, while the $OH^-$ ions from the portlandite diffused outwards and reacted with the $Mg^{2+}$ ions invading inwards the crack to form brucite. At the same time, the remaining $Ca^{2+}$ ions reacted with $CO_3^{2-}$ to form calcite, which also contributes to the crack closure. To efficiently block the pathway in the crack and to hinder the further ingress of aggressive ions, precipitates must form inside the crack space, particularly in the crack mouth，rather than inside the broken capsules. According to the mineralogy of the reaction products of these two agents (see Fig. 4), the percentage of portlandite is higher in the reaction products of CaO-$NaAlO_2$ self-healing which could support an efficient distribution of reaction products in the crack and in particular also the formation of calcite. Thus, although the volume increase of CaO-$NaAlO_2$ agent reacting with sea water is lower, the effect of CaO-$NaAlO_2$ agent on crack closure could be better than that of CaO-metakaolin agent. Further studies will be necessary to clarify this point.

Moreover, the volume increase of the self-healing agents in simulated sea water underline the slower reaction of metakaolin compared to the $NaAlO_2$ agent and this will also affect the kinetics of the binding of aggressive ions. In fact, the kinetic of the volume increase of the self-healing agents (Fig. 14) agree well with the kinetics of ion

binding, i.e. the removal efficiency (Fig. 12) and the mass percentages of ions chemically bound in the reaction products (Fig. 13). The aim of this study was to design a self-healing agent that is not only able to close cracks, but also to chemically bind chloride, sulfate and magnesium in sea water. The faster reactions of CaO-$NaAlO_2$ agent lead to faster chemical binding. In addition, the corresponding pH in the solution is higher than that with CaO-metakaolin agent, which more efficiently lowers the $[Cl^-]/[OH^-]$ ratio. From this point of view, as discussed in Section 3.1.3, CaO-$NaAlO_2$ agent will be more efficient for mitigation on corrosion of steel bars, although its chloride binding is slightly lower than that of CaO-metakaolin.

In this study, the reactions of self-healing agents took place directly in seawater. The influence of the pore solution of the bulk matrix on the reaction process of self-healing agents was ignored. Because of the higher concentrations and larger diffusion coefficients, $OH^-$ and $Ca^{2+}$ are the ions from the pore solution that may influence the composition of the crack solution, rather than the other ions in the pore solution. It must be mentioned that, however, compared with the direct dissolution of the self-healing agent, which could be stored in capsules and exposed to the crack solution after the capsules were intersected by the crack, the diffusion of $OH^-$ and $Ca^{2+}$ ions from the pore solution are too slow to influence the reactions of self-healing agents. Therefore, the studies on the reactions of self-healing agents directly taking place in seawater here can still provide useful information for understanding the self-healing of cracks in cement-based materials.

## 4. Conclusion

In this study, thermodynamics and kinetics of the reaction of Ca-Al self-healing agents and chemical binding of aggressive ions in sea water were investigated. Based on the experimental and thermodynamic modeling results, following conclusions can be drawn:

(1) According to the thermodynamic modeling, the formation of Friedel's salt, Kuzel's salt, ettringite and hydrotalcite indicates that Ca-Al self-healing agents can chemically bind aggressive ions in sea water. Moreover, the Ca/Al molar ratio of self-healing

agents has significant effects on the mineralogy of the phase assemblages.

(2) Both for CaO-$NaAlO_2$ and CaO-metakaolin agents the removal efficiency of $Cl^-$ ions firstly increases and then decreases with Ca/Al, while the removal efficiency of $Mg^{2+}$ and $SO_4^{2-}$ ions are hardly influenced by Ca/Al and near to 100%. The molar Ca/Al ratios corresponding to the maximum removal efficiency of $Cl^-$ ion in CaO-$NaAlO_2$ and CaO-metakaolin agents was approximately 3 as determined by means of thermodynamic modeling. The pH of the solutions with CaO-$NaAlO_2$ and CaO-metakaolin agents at Ca/Al = 3, respectively, is higher than 13 when the agent to water ratio is larger than 0.2.

(3) The kinetics of chemical reaction between self-healing agents and simulated sea water was investigated via XRD and solution analysis. For CaO-$NaAlO_2$ agent it was found that $NaAlO_2$ can rapidly dissolve in water and release $Al(OH)_4^-$, making precipitates formed very fast. For the CaO-metakaolin agent, portlandite formed within the first 12 hours, while the reaction of metakaolin, which make aggressive ions in sea water bound, occurred mainly after more than 3 days. Because of the faster reaction and higher pH enhancement of CaO-$NaAlO_2$ agent, the $[Cl^-]/[OH^-]$, which is an indicator to corrosion risk of steel bars, would be much lower in the crack solution than that for CaO-metakaolin agent. From this point of view, CaO-$NaAlO_2$ agent will be more efficient for declining the corrosion risk of steel bars in cracked concrete.

(4) For magnesium and chloirde, the removal efficiencies determined by solution analysis compared well with those determined via thermodynamic modeling, while for sulfate$^-$ the experimental removal efficiency was lower than predicted by thermodynamic modeling.

(5) For CaO-$NaAlO_2$ agent mixed with sea water, the volume of the solid phase increases dramatically within the first 12 hours. For the CaO-metakaolin agent, volume increase experiences two stages due to the hydration of lime and the pozzolanic reaction of metakaolin, respectively.

In summary the investigated self-healing agents can bind chloride, magnesium and sulfate very efficiently and in both cases additional volume was generated due to the hydration reaction; the $NaAlO_2$ based agent showed a faster kinetic than the

CaO-metakaolin agent.


## Acknowledgement

The financial support of the Ministry of Science and Technology of the People's Republic of China National Key R&D Program of China (No. 2017YFB0309904), the National Natural Science Foundation of China (No. 51602050 and No. 51872097), Open Fund Project of State Key Laboratory of Silicate Materials for Architectures (Wuhan University of Technology) (No.YSJJ2020-09) and Key Laboratory of Advanced Civil Engineering Materials of Ministry of Education (Tongji University) (No. 202005)is greatly appreciated.


## Reference


[1] H. Huang, G. Ye, C. Qian, E. Schlangen, Self-healing in cementitious materials: Materials, methods and service conditions, Materials & Design, 92 (2016) 499-511.

[2] K. Van Tittelboom, N. De Belie, Self-healing in cementitious materials—A review, Materials, 6 (2013) 2182-2217.

[3] H.M. Jonkers, Self healing concrete: a biological approach, in: Self healing materials, Springer, 2007, pp. 195-204.

[4] M. Seifan, A.K. Samani, A. Berenjian, Bioconcrete: next generation of self-healing concrete, Applied microbiology and biotechnology, 100 (2016) 2591-2602.

[5] W. Li, B. Dong, Z. Yang, J. Xu, Q. Chen, H. Li, F. Xing, Z. Jiang, Recent Advances in Intrinsic Self‐Healing Cementitious Materials, Advanced materials, 30 (2018) 1705679.

[6] H. Liu, H. Huang, X. Wu, H. Peng, Z. Li, J. Hu, Q. Yu, Effects of external multi-ions and wet-dry cycles in a marine environment on autogenous self-healing of cracks in cement paste, Cement and Concrete Research, 120 (2019) 198-206.

[7] X. Wu, H. Huang, H. Liu, Z. Zeng, H. Li, J. Hu, J. Wei, Q. Yu, Artificial aggregates for self-healing of cement paste and chemical binding of aggressive ions from sea water, Composites Part B: Engineering, (2019) 107605.

[8] M. Otieno, H. Beushausen, M. Alexander, Chloride-induced corrosion of steel in cracked concrete–Part I: Experimental studies under accelerated and natural marine environments, Cement

and Concrete Research, 79 (2016) 373-385.
[9] B. Van Belleghem, S. Kessler, P. Van den Heede, K. Van Tittelboom, N. De Belie, Chloride induced reinforcement corrosion behavior in self-healing concrete with encapsulated polyurethane, Cement and Concrete Research, 113 (2018) 130-139.
[10] W.G. Valencia Saavedra, D.E. Angulo, R. Mejia de Gutierrez, Fly ash slag geopolymer concrete: Resistance to sodium and magnesium sulfate attack, Journal of Materials in Civil Engineering, 28 (2016) 04016148.
[11] Z. Shi, M.R. Geiker, K. De Weerdt, T.A. Østnor, B. Lothenbach, F. Winnefeld, J. Skibsted, Role of calcium on chloride binding in hydrated Portland cement–metakaolin–limestone blends, Cement and Concrete Research, 95 (2017) 205-216.
[12] W. Kunther, B. Lothenbach, J. Skibsted, Influence of the Ca/Si ratio of the C–S–H phase on the interaction with sulfate ions and its impact on the ettringite crystallization pressure, Cement and concrete research, 69 (2015) 37-49.
[13] A. Machner, M. Zajac, M.B. Haha, K.O. Kjellsen, M.R. Geiker, K. De Weerdt, Limitations of the hydrotalcite formation in Portland composite cement pastes containing dolomite and metakaolin, Cement and Concrete Research, 105 (2018) 1-17.
[14] H. Huang, G. Ye, D. Damidot, Characterization and quantification of self-healing behaviors of microcracks due to further hydration in cement paste, Cement and Concrete Research, 52 (2013) 71-81.
[15] X. Wu, H. Huang, H. Liu, Z. Zeng, H. Li, J. Hu, J. Wei, Q. Yu, Artificial aggregates for self-healing of cement paste and chemical binding of aggressive ions from sea water, Composites Part B: Engineering, 182 (2020) 107605.
[16] L. Lv, P. Guo, G. Liu, N. Han, F. Xing, Light induced self-healing in concrete using novel cementitious capsules containing UV curable adhesive, Cement and Concrete Composites, 105 (2020) 103445.
[17] B. Hilloulin, K. Van Tittelboom, E. Gruyaert, N. De Belie, A. Loukili, Design of polymeric capsules for self-healing concrete, Cement and Concrete Composites, 55 (2015) 298-307.
[18] B. Lothenbach, D.A. Kulik, T. Matschei, M. Balonis, L. Baquerizo, B. Dilnesa, G.D. Miron, R.J. Myers, Cemdata18: A chemical thermodynamic database for hydrated Portland cements and alkali-activated materials, Cement and Concrete Research, 115 (2019) 472-506.
[19] B. Lothenbach, Thermodynamic equilibrium calculations in cementitious systems, Materials and

624 Structures, 43 (2010) 1413-1433.
625 [20] B. Huet, V. L’ Hostis, F. Miserque, H. Idrissi, Electrochemical behavior of mild steel in concrete:
626 Influence of pH and carbonate content of concrete pore solution, Electrochimica Acta, 51 (2005)
627 172-180.
628 [21] B. Huet, V. L'Hostis, L. Tricheux, H. Idrissi, Influence of alkali, silicate, and sulfate content of
629 carbonated concrete pore solution on mild steel corrosion behavior, Materials and Corrosion, 61 (2009)
630 111-124.
631 [22] D.A. Hausmann, STEEL CORROSION IN CONCRETE -- HOW DOES IT OCCUR?, Materials protection,
632 (1967).
633 [23] G. Liu, Y. Zhang, Z. Ni, R. Huang, Corrosion behavior of steel submitted to chloride and sulphate
634 ions in simulated concrete pore solution, Construction and Building Materials, 115 (2016) 1-5.
635 [24] V. Shah, K. Scrivener, B. Bhattacharjee, S. Bishnoi, Changes in microstructure characteristics of
636 cement paste on carbonation, Cement and Concrete Research, 109 (2018) 184-197.
637 [25] T. Matschei, B. Lothenbach, F.P. Glasser, Thermodynamic properties of Portland cement hydrates
638 in the system CaO–Al2O3–SiO2–CaSO4–CaCO3–H2O, Cement and Concrete Research, 37 (2007)
639 1379-1410.
640 [26] W. Stumm, J.J. Morgan, Chemical Equilibria and Rates in Natural Waters, Aquatic Chemistry,
641 (1996).
642 [27] B. Lothenbach, G. Furrer, Scharli, Helen, R. Schulin, Immobilization of Zinc and Cadmium by
643 Montmorillonite Compounds: Effects of Aging and Subsequent Acidification, Environmental Science &
644 Technology, 33 (1999) 2945-2952.
645 [28] G. Wang, Y. Wang, Z. Gao, Use of steel slag as a granular material: volume expansion prediction
646 and usability criteria, Journal of Hazardous Materials, 184 (2010) 555-560.
647 [29] S. Nagataki, H. Gomi, Expansive admixtures (mainly ettringite), Cement and concrete composites,
648 20 (1998) 163-170.

649 Table 1. Chemical equations and the corresponding equilibrium constants at 25°C [18,
650 19]

| Minerals | Chemical equations | log $K_{so}$ |
|---|---|---|
| Ettringite | $3CaO \cdot Al_2O_3 \cdot 3CaSO_4 \cdot 32H_2O \Leftrightarrow 6Ca^{2+} + 2Al(OH)_4^- + 3SO_4^{2-} + 4OH^- + 26H_2O$ | -44.9 |
| Friedel's salt | $3CaO \cdot Al_2O_3 \cdot CaCl_2 \cdot 10H_2O \Leftrightarrow 4Ca^{2+} + 2Al(OH)_4^- + 2Cl^- + 4OH^- + 4H_2O$ | -27.3 |
| Hydrotalcite | $Mg_4Al_2(OH)_{14} \cdot 3H_2O \Leftrightarrow 2Al(OH)_4^- + 4Mg^{2+} + 6OH^- + 3H_2O$ | -56.0 |
| CSHQ-JenD | $1.5CaO \cdot 0.6667SiO_2 \cdot 2.5H_2O + 3H^+ \Leftrightarrow 1.5Ca^{2+} + 4H_2O + 0.6667SiO_2$ | 28.7 |
| CSHQ-JenH | $1.3333CaO \cdot SiO_2 \cdot 2.1667H_2O + 2.6666H^+ \Leftrightarrow 1.3333Ca^{2+} + 3.5H_2O + SiO_2$ | 22.2 |
| CSHQ-TobD | $0.6667(1.25\ CaO \cdot SiO_2 \cdot 2.75H_2O) + 1.66675H^+ \Leftrightarrow 0.833375Ca^{2+} + 2.6668H_2O + 0.6667SiO_2$ | 13.7 |
| CSHQ-TobH | $0.6667CaO \cdot SiO_2 \cdot 1.5H_2O + 1.3334H^+ \Leftrightarrow 0.6667Ca^{2+} + 2.1667H_2O + SiO_2$ | 8.3 |
| $C_3AH_6$ | $Ca_3Al_2(OH)_{12} \Leftrightarrow 3Ca^{2+} + 2Al(OH)_4^- + 4OH^-$ | -20.5 |
| Kuzel's salt | $Ca_4Al_2Cl\ (SO_4)_{0.5}\ (OH)_{12} \cdot 6H_2O \Leftrightarrow 4Ca^{2+} + 2Al(OH)_4^- + Cl^- + 0.5SO_4^{2-} + 4OH^- + 6H_2O$ | -28.5 |
| Natrolite | $Na_2Al_2Si_3O_{10} \cdot 2H_2O \Leftrightarrow 2Na^+ + 2Al(OH)_4^- + 3SiO_2 + 2H_2O$ | -30.2 |
| Straetlingite | $Ca_4Al_2SiO_2(OH)_{10} \cdot 3H_2O \Leftrightarrow 2Ca^{2+} + 2Al(OH)_4^- + SiO(OH)_3^- + OH^- + 2H_2O$ | -19.7 |
| Portlandite | $Ca(OH)_2 \Leftrightarrow Ca^{2+} + 2OH^-$ | -5.2 |
| Cacite | $CaCO_3 \Leftrightarrow CO_3^{2-} + Ca^{2+}$ | -3.2 |
| Brucite | $Mg(OH)_2 + 2H^+ \Leftrightarrow Mg^{2+} + 2H_2O$ | 16.8 |

| | | |
|---|---|---|
| Monocarbonate | $Ca_4Al_2CO_9(H_2O)_{11} + 4H^+ \Leftrightarrow 2AlO_2^- + CO_3^{2-} + 4Ca^{2+} + 13H_2O$ | 24.5 |
| Hemicarbonate | $(CaO)_3Al_2O_3(CaCO_3)_{0.5}(CaO_2H_2)_{0.5}(H_2O)_{11.5} + 5H^+ \Leftrightarrow 2AlO_2^- + 0.5CO_3^{2-} + 4Ca^{2+} + 14.5H_2O$ | 40.9 |

651

652

653

654

655

656

657 Table 2. Compounds used to prepare sea water and the main ion concentrations in the simulated

658 sea water with pH=7.3

| Compounds used to synthesize sea water | Dosage [g/L] | Ions in simulated sea water | Concentration [g/L] |
|---|---|---|---|
| $NaHCO_3$ | 0.19 | $Cl^-$ | 19.36 |
| $CaCl_2 \cdot 2H_2O$ | 1.47 | $Mg^{2+}$ | 1.27 |
| $MgCl_2 \cdot 6H_2O$ | 10.57 | $SO_4^{2-}$ | 2.69 |
| $Na_2SO_4 \cdot 10H_2O$ | 9.02 | $Ca^{2+}$ | 0.40 |
| KCl | 0.75 | $Na^+$ | 10.82 |
| NaCl | 24.08 | $K^+$ | 0.39 |
| | | $HCO_3^-$ | 0.14 |

659

660

661

662

663 Table 3. Contents of crystalline phases in reaction products of self-healing agent
664 reacted with seawater for 28 days

| Crystals / Self-healing agents | F/H/S (% b.w.) | $Ca(OH)_2$ (% b.w.) | $CaCO_3$ (% b.w.) | $R_w$ | sig |
|---|---|---|---|---|---|
| $CaO/NaAlO_2$ (Ca/Al=3) | 66±3.3 | 28±1.4 | 6±0.3 | 9.56 | 1.82 |
| $CaO/NaAlO_2$ (Ca/Al=5) | 47±2.4 | 50±2.5 | 3±0.1 | 11.05 | 2.02 |
| CaO-metakaolin (Ca/Al=5) | 52±2.6 | 28±1.4 | 20±1.0 | 12.12 | 2.12 |

665 Note: For the reaction, the ratio between the mass of self-healing agent and the mass of sea
666 water was 0.2.
667

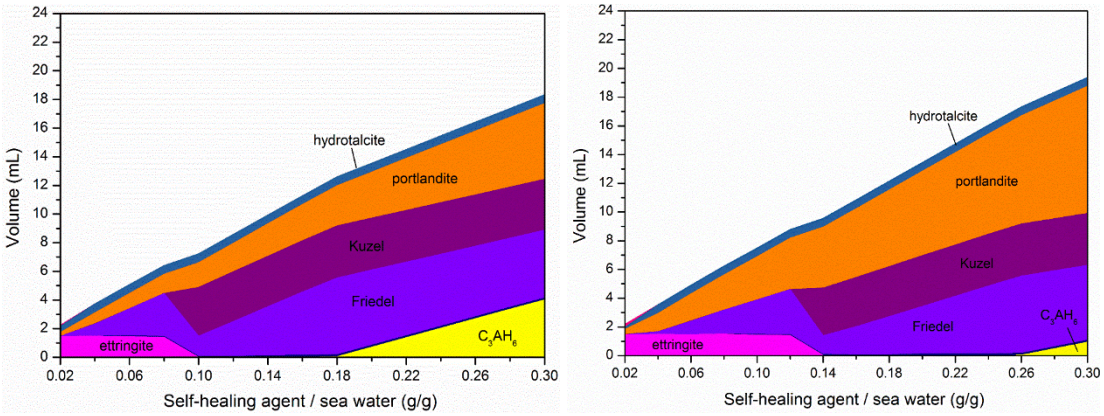


(a) (b)

Fig. 1 Phase assemblages in the mixture of CaO-$NaAlO_2$ and 100 ml sea water based on thermodynamic modeling: (a) with Ca/Al molar ratio of 3; (b) with Ca/Al molar ratio of 5

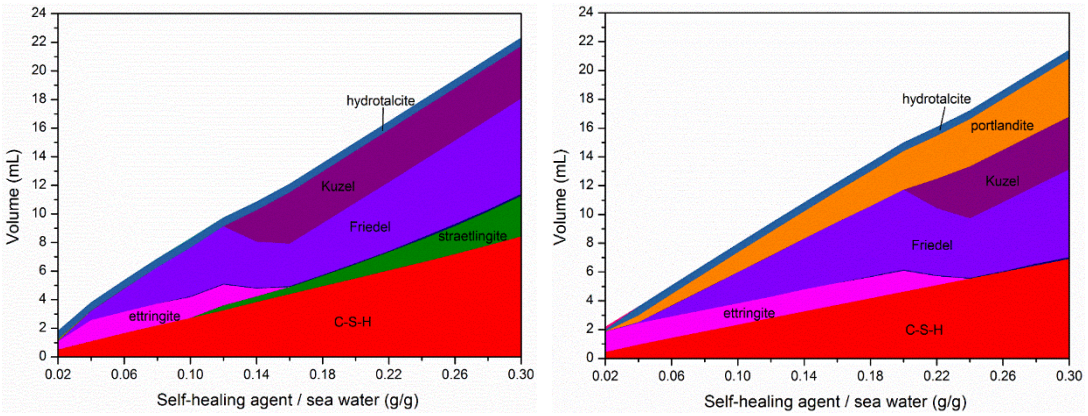


(a) (b)

Fig. 2 Phase assemblages in the mixture of CaO-metakaolin and 100 ml sea water based on thermodynamic modeling: (a) with Ca/Al molar ratio of 3; (b) with Ca/Al molar ratio of 5

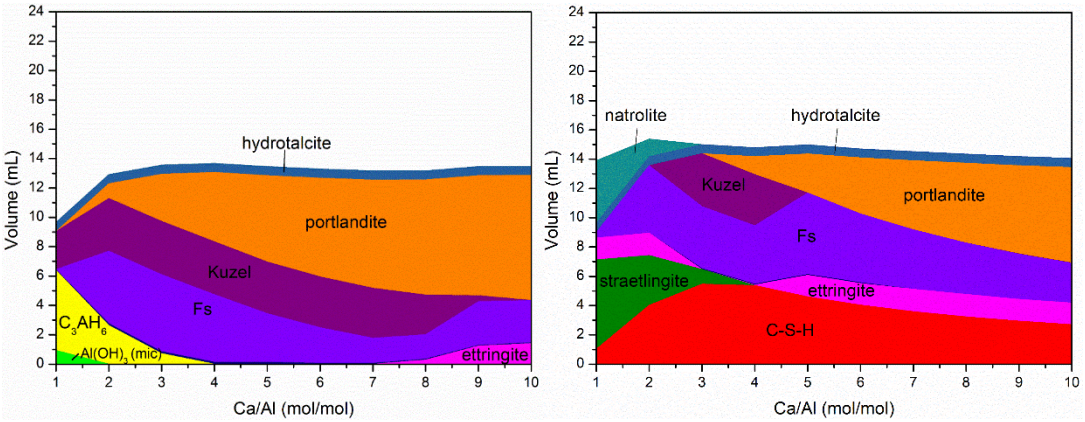


(a) (b)

Fig. 3 Phase assemblages in the mixture of 100 ml sea water and 20 g self-healing agents with various Ca/Al based on thermodynamic modeling: (a) $CaO\text{-}NaAlO_2$; (b) CaO-metakaolin. Fs: Friedel's salt

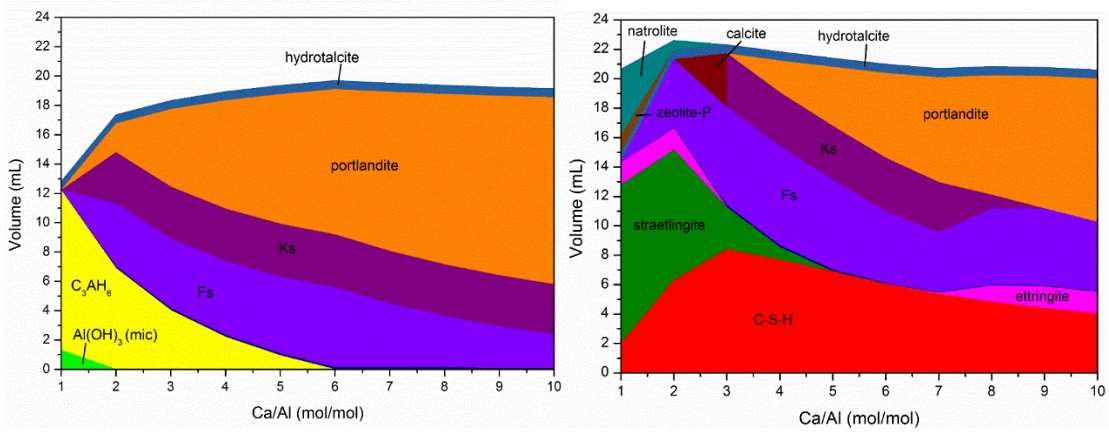


(a) (b)

Fig. 4 Phase assemblages in the mixture of 100 ml sea water and 30 g self-healing agents with various Ca/Al based on thermodynamic modeling: (a) $CaO\text{-}NaAlO_2$; (b) CaO-metakaolin. Fs: Friedel's salt; Ks: Kuzel's salt

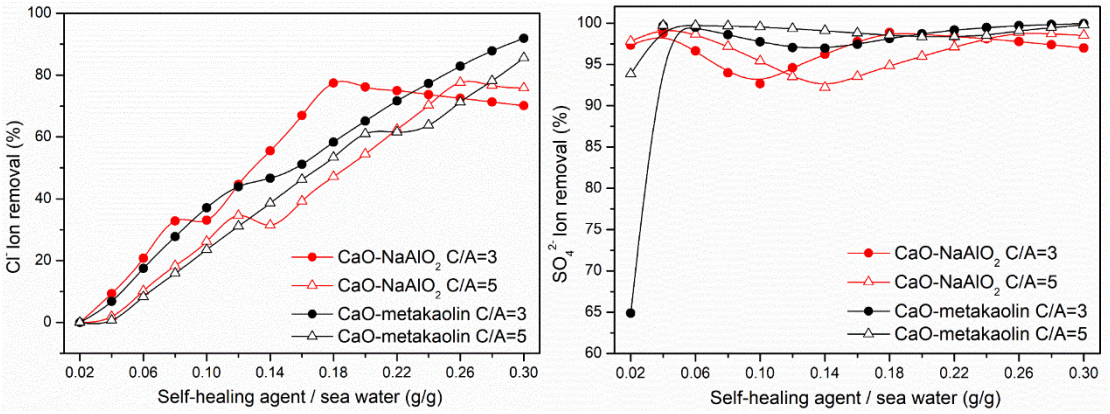


(a) (b)

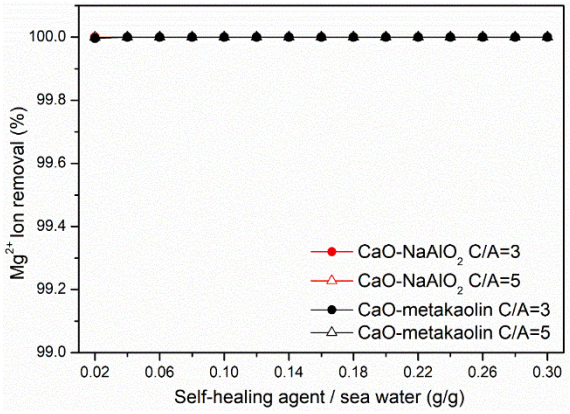


(c)

Fig. 5 Removal efficiency of ions as a function of ratio between the mass of agent to the mass of sea water based on thermodynamic modeling: (a) $Cl^-$; (b) $SO_4^{2-}$; (c) $Mg^{2+}$ in sea water. C/A means Ca/Al molar ratio.

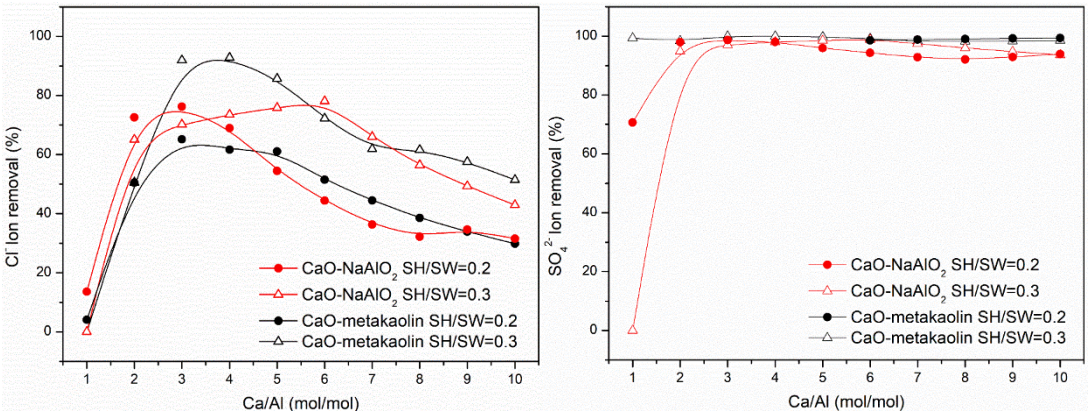


(a) (b)

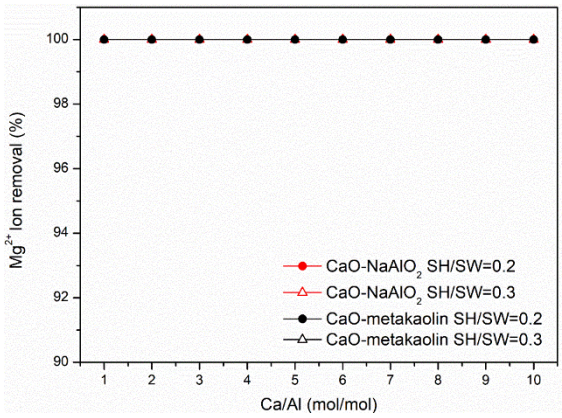


(c)

Fig. 6 Removal efficiency of chloride, sulfate and magnesium in sea water as a function of Ca/Al in self-healing agents based on thermodynamic modeling: (a) $Cl^-$; (b) $SO_4^{2-}$; (c) $Mg^{2+}$. SH/SW refers to the ratio between the mass of self-healing agent and the mass of sea water.

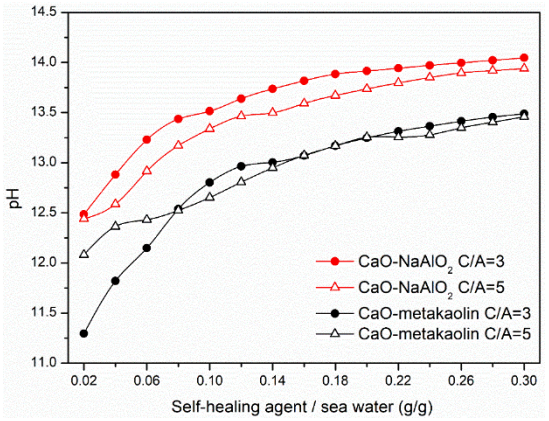


Fig. 7 pH value as a function of the ratio between the mass of agent to the mass of sea water based on thermodynamic modeling. C/A means Ca/Al molar ratio.

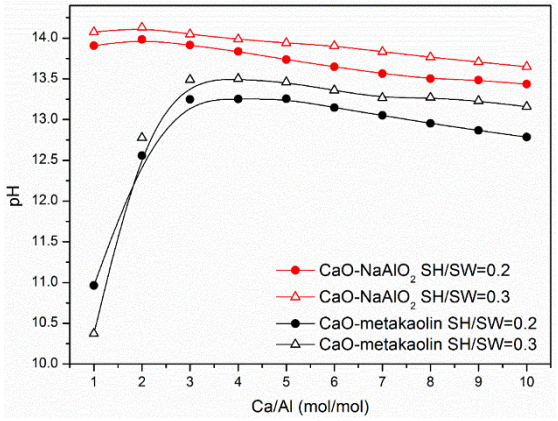


Fig. 8 pH value in sea water mixed with self-healing agent with various Ca/Al based on thermodynamic modeling. SH/SW refers to the ratio between the mass of self-healing agent and the mass of sea water.

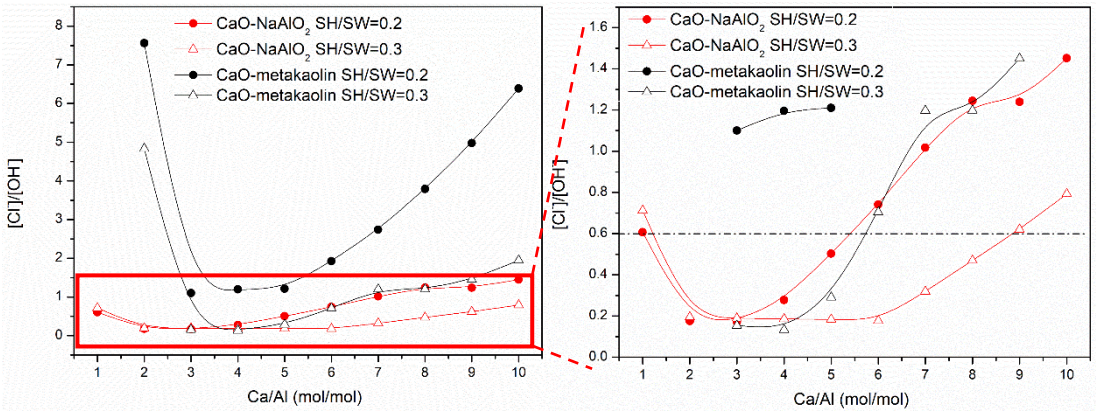


(a)

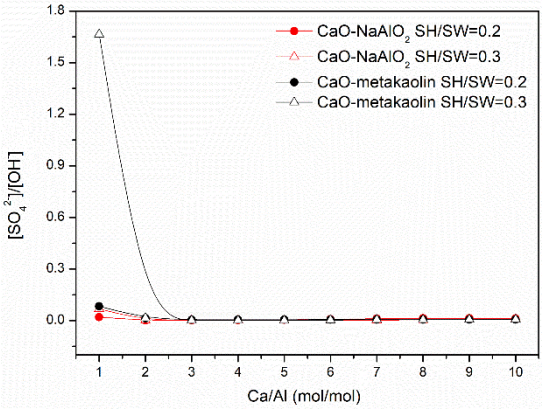


(b)

Fig. 9 Ratios between concentration of $Cl^-$ or $SO_4^{2-}$ and the concentration of $OH^-$: (a) $Cl^-/OH^-$, (b) $SO_4^{2-}/OH^-$. SH/SW refers to the ratio between the mass of self-healing agent and the mass of sea water.

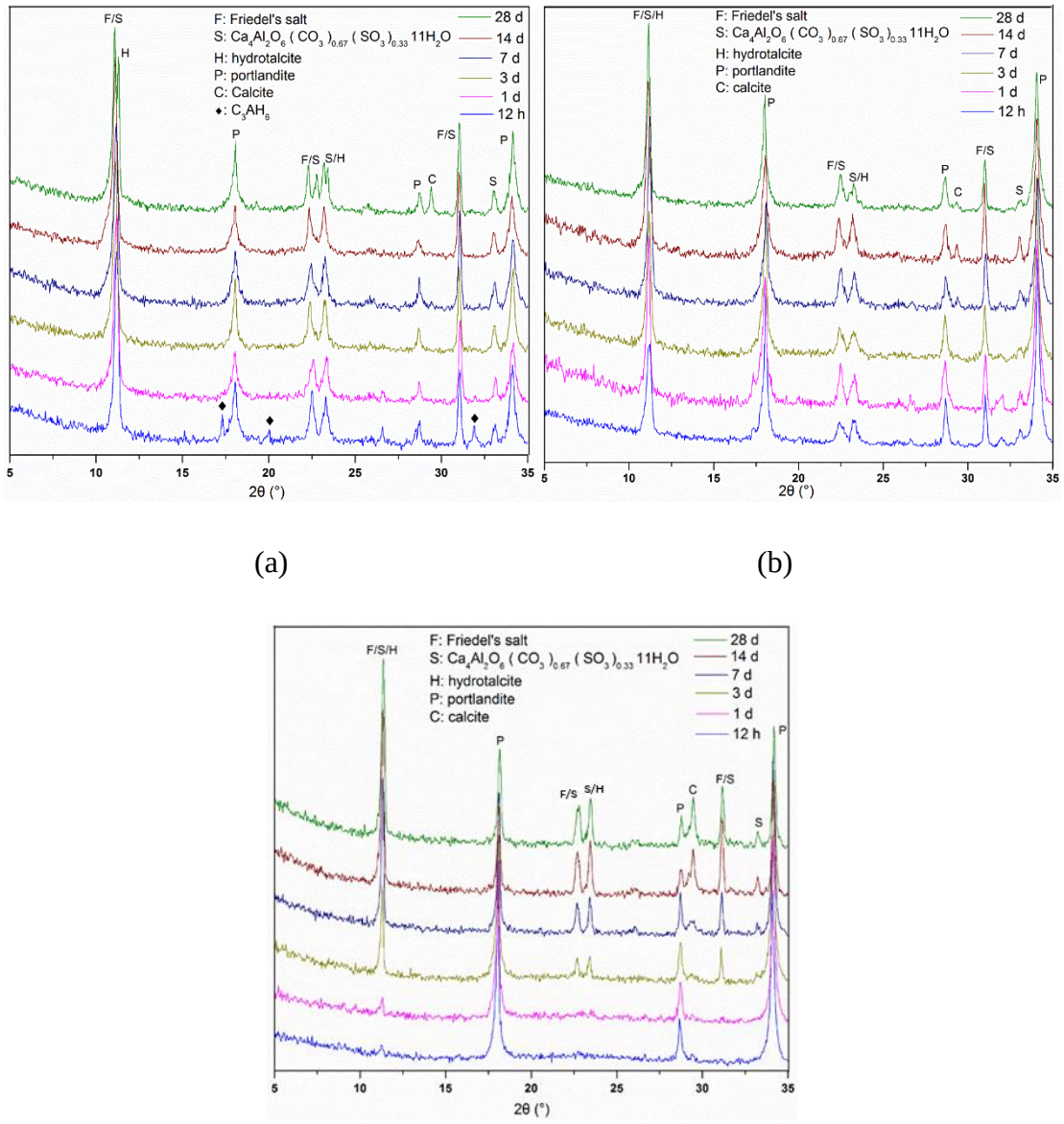


Fig. 10 XRD patterns of solid phases obtained after the reaction of the self-healing agent with sea water: (a) CaO-$NaAlO_2$ agent with Ca/Al of 3; (b) CaO-$NaAlO_2$ agent with Ca/Al of 5; (c) CaO-metakaolin agent with Ca/Al of 5. For reactions, the ratio between the mass of self-healing agent and the mass of sea water was 0.2.

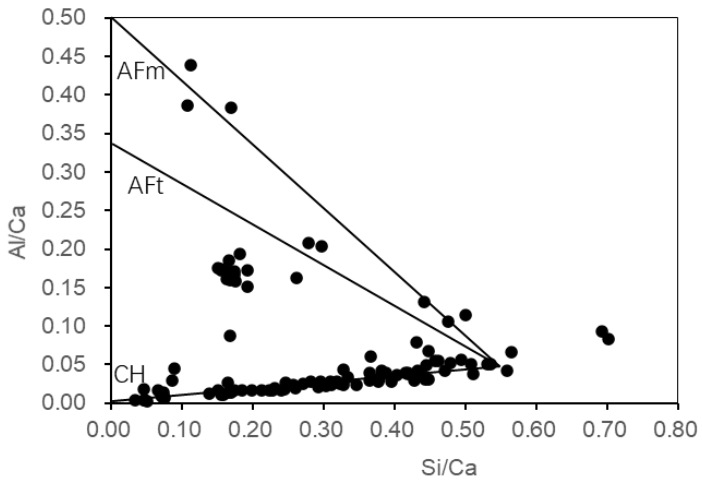


Fig. 11 EDS point analysis of reaction products of CaO-metakaolin reacted with seawater for 28 days. For the reaction, the ratio between the mass of self-healing agent and the mass of sea water was 0.2.

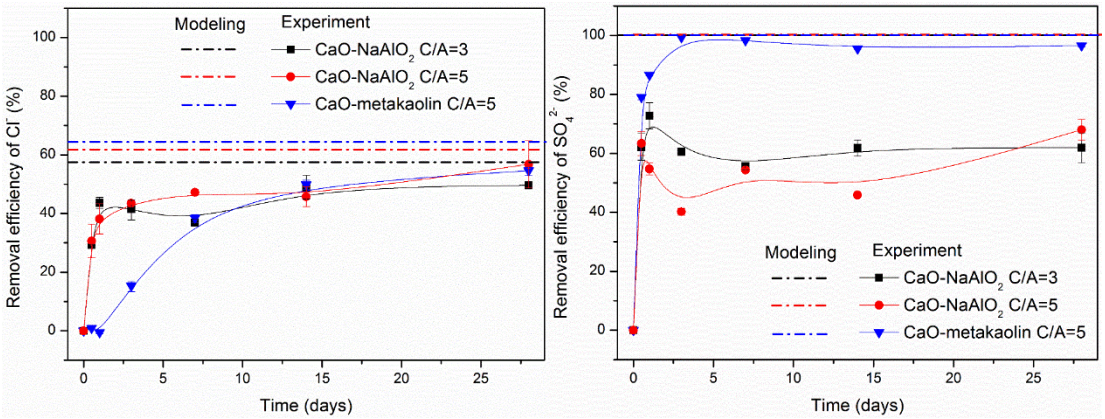


(a) (b)

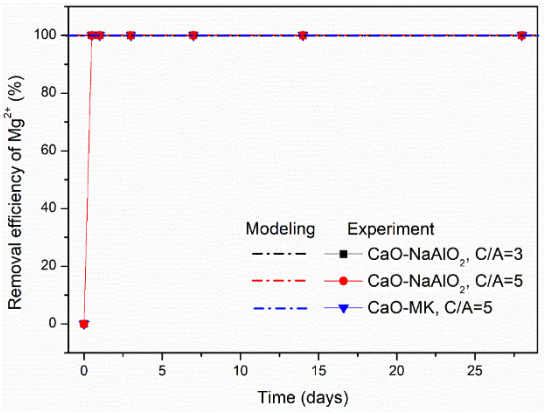


(c)

Fig. 12 Removal efficiency of aggressive ions in sea water after reaction with self-healing agents for different periods: (a) $Cl^-$; (b) $SO_4^{2-}$; (c) $Mg^{2+}$. C/A means Ca/Al molar ratio.

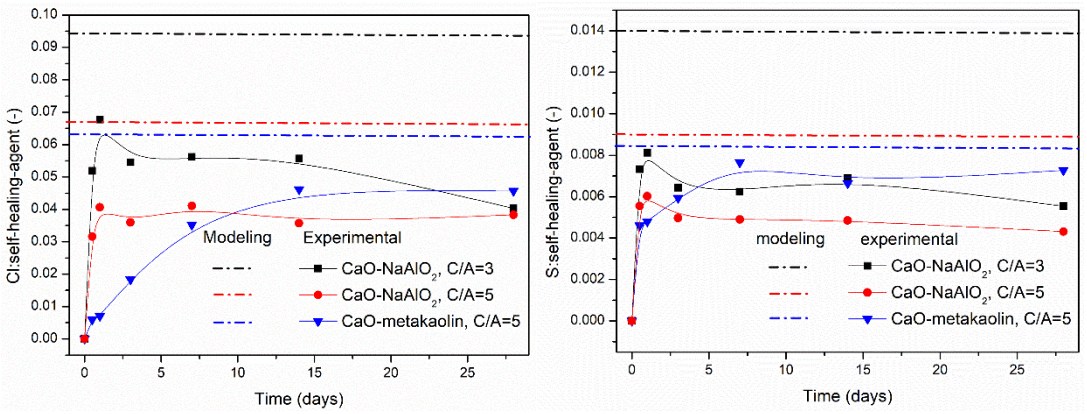


(a) (b)

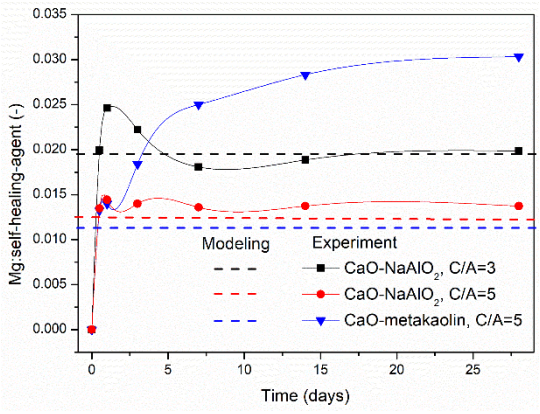


(c)

Fig. 13 Aggressive ions binding efficiency in reaction products: (a) $Cl^-$; (b) $SO_4^{2-}$; (c) $Mg^{2+}$. C/A means Ca/Al molar ratio.

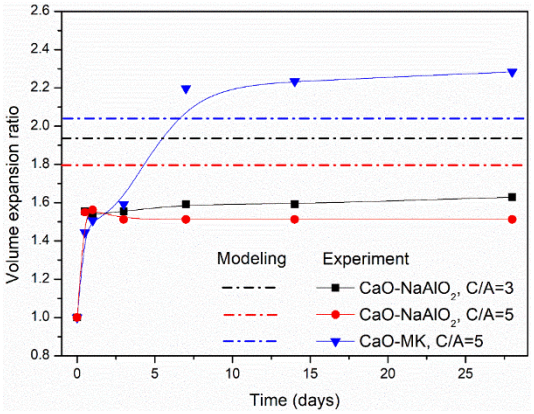


Fig. 14 Volume increase ratio of self-healing agents mixed with simulated sea water. C/A means Ca/Al molar ratio.

**Conflict of interest**

The authors declared that they have no conflicts on interest to this work.